Proc. Natl. Acad. Sci. USA
Vol. 94, pp. 14889–14893, December 1997
Neurobiology

Hair cell-specific splicing of mRNA for the α_{1D} subunit of voltage-gated Ca^{2+} channels in the chicken's cochlea

RICHARD KOLLMAR, JOHN FAK, LISA G. MONTGOMERY*, AND A. J. HUDSPETH†

Howard Hughes Medical Institute and Laboratory of Sensory Neuroscience, The Rockefeller University, New York, NY 10021-6399

Contributed by A. J. Hudspeth, October 24, 1997

ABSTRACT **The L-type voltage-gated Ca^{2+} channels that control tonic release of neurotransmitter from hair cells exhibit unusual electrophysiological properties: a low activation threshold, rapid activation and deactivation, and a lack of Ca^{2+}-dependent inactivation. We have inquired whether these characteristics result from cell-specific splicing of the mRNA for the L-type α_{1D} subunit that predominates in hair cells of the chicken's cochlea. The α_{1D} subunit in hair cells contains three uncommon exons: one encoding a 26-aa insert in the cytoplasmic loop between repeats I and II, an alternative exon for transmembrane segment IIIS2, and a heretofore undescribed exon specifying a 10-aa insert in the cytoplasmic loop between segments IVS2 and IVS3. We propose that the alternative splicing of the α_{1D} mRNA contributes to the unusual behavior of the hair cell's voltage-gated Ca^{2+} channels.**

Although classified as L-type on pharmacological grounds, the hair cell's voltage-gated Ca^{2+} channels display unusual electrophysiological behavior. These channels open at more negative membrane potentials than most L-type channels, between −60 mV and −45 mV; they open and close an order of magnitude faster, with time constants of 0.1–0.5 ms; and they do not inactivate in a voltage- or Ca^{2+}-dependent manner over hundreds of milliseconds (1, 2). These characteristics enable a hair cell to respond rapidly to a protracted stimulus of varying intensity and to transmit information about its amplitude, frequency, and phase across a tonic synapse (reviewed in ref. 3).

The unusual properties of the hair cell's voltage-gated Ca^{2+} conductance could result from cell-specific modification of an L-type channel. Whereas the drug sensitivity and permeability of a voltage-gated Ca^{2+} channel depend on its type of pore-forming α_1 subunit, the channel's gating depends on the specific combination of the α_1 subunit and four to five auxiliary subunits (reviewed in refs. 4 and 5). Alternative splicing creates additional diversity, but its functional consequence is known for only a few variants (6, 7).

We have previously shown that most, if not all, voltage-gated Ca^{2+} channels in hair cells of the chicken's cochlea contain the ortholog of the mammalian L-type α_{1D} subunit (8). To understand how these Ca^{2+} channels are adapted to fast and tonic synaptic transmission, we investigated whether the mRNA specifying this α_{1D} subunit is alternatively spliced.

MATERIALS AND METHODS

PCR Analysis of Splice Isoforms. RNA isolation, cDNA synthesis, PCR amplification, DNA sequencing, and Southern blotting of PCR products were conducted as described (8). Hair cells from the sacculus of the bullfrog, *Rana catesbeiana*, were obtained as described (9). Sequences were compared with consensus matrices with MATIND and MATINSPECTOR software (10).

The primers around the I-II-loop insert were (Fig. 1*A*): F_9, TGATGAAGAAGGGAAACGGA; F_{9a}, AAGGGAAACGGAACAGGGTT; F_{10}, AAGGGAAACGGAACACAAGC; and R_{14}, CAGGTGAACAAAGCCAGAAGAA; the internal probe was TGTAGAGCTGCAGTAAAATCTGTC. Around the IIIS2 segment, the primers were (Fig. 1*B*): F_{20}, GGAGTGCCTTCTTCATTTTCA; P_{21}, AGGCTCATCAATCACCACATC; R_{22}, AAACATACTAGTGAAGACATAATCTGCA; R_{22a}, GGCTGTGAAAGCATAGTCAAAG; and R_{25}, TACAAGCAAACATGAACTGCA. Around the IVS2–3 insert, the primers were (Fig. 1*C*): F_{30}, AGCTGATTGCATTCAAACCC; F_{30a}, TGATTGCATTCAAACCCAAGAT; F_{31}, ATTGCATTCAAACCCAAGGG; F_{31a}, ATTGCATTCAAACCCAAGCA; and R_{33}, CACTCGGAAAAGACGGAAAAA; the internal probe was AGCGCAAGAATCTCCATCAC.

To amplify products longer than 2 kb, we used a combination of *Taq* and *Pwo* DNA polymerases (Expand Long Template PCR System, Boehringer Mannheim) and the following primers: exon 2 forward, AAACGCCAGCAATATGCCAAGAGC; exon 9 forward, ATGAAGAGGCTGATGAAGAAGGGAAACG; exon 9a reverse, TGTTTATTGGAAGACCGGCCAAAGC; exon 10 reverse, TGACTCGGTTTCGCTGGTGGG; exon 21 reverse, TTCTGCTGCTAGGGAAACACTGCTCA; and exon 37 reverse, CCAAATGATGAGGACCCAGAATGGA.

Antibody Purification. The I-II loops (amino acids 401–545) from clones pSE9/39–1 and pBr17 (8), respectively with and without the alternatively spliced insert, were subcloned between the *Eco*RI and *Xho*I sites of the expression plasmid pET-21a(+) (Novagen). The resulting fusion proteins with 16 aa at their amino termini, including a T7 tag, and 8 aa at their carboxyl termini, including a $(His)_6$ tag, were expressed in the host *Escherichia coli* BL21(DE3) and purified under denaturing conditions by affinity chromatography on immobilized Ni^{2+}. The purified protein with the insert precipitated from the eluate upon dialysis against PBS (138 mM NaCl, 2.7 mM KCl, and 10 mM sodium phosphate at pH 7.4) and was used without further conjugation to immunize rabbits (Pel-Freez Biologicals). The synthetic peptide (Research Genetics, Huntsville, AL) CRVTLADLMEEKKKSRLS, which represents a part of the I-II-loop insert, and CSGEGENPASSGSLSQT, which represents a part of the I-II loop that is conserved among α_{1D} subunits, were coupled to iodoacetyl-agarose columns (SulfoLink, Pierce). Antibodies specific for either epitope were affinity-purified on these antigen columns as described (11).

Protein Immunoblotting. Fusion proteins expressed in bacteria were separated in a gradient gel containing 10–20% (wt/vol) polyacrylamide in Tris·glycine buffer solution with

The publication costs of this article were defrayed in part by page charge payment. This article must therefore be hereby marked "*advertisement*" in accordance with 18 U.S.C. §1734 solely to indicate this fact.

*Present address: Department of Pharmacology, University of Texas Southwestern Medical Center, Dallas, TX 75235.
†To whom reprint requests should be addressed. e-mail: hudspaj@rockvax.rockefeller.edu.

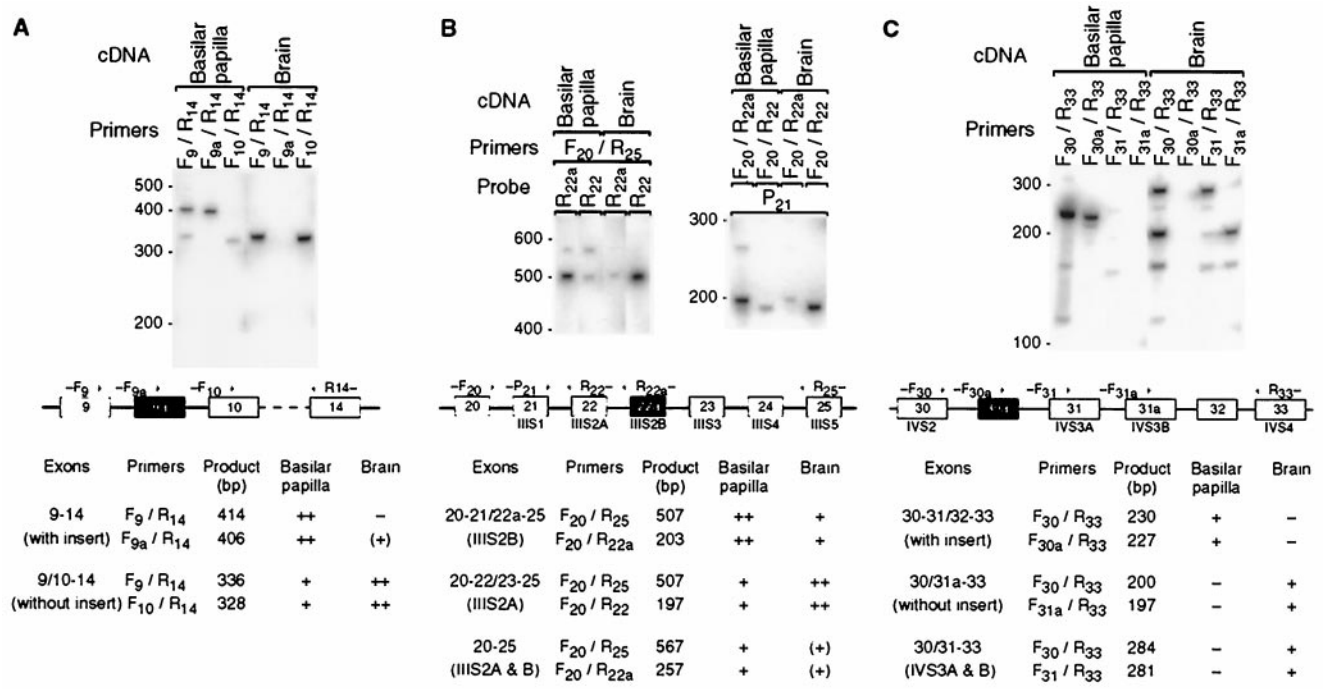

Exons	Primers	Product (bp)	Basilar papilla	Brain
9-14	F_9 / R_{14}	414	++	–
(with insert)	F_{9a} / R_{14}	406	++	(+)
9/10-14	F_9 / R_{14}	336	+	++
(without insert)	F_{10} / R_{14}	328	+	++

Exons	Primers	Product (bp)	Basilar papilla	Brain
20-21/22a-25	F_{20} / R_{25}	507	++	+
(IIIS2B)	F_{20} / R_{22a}	203	++	+
20-22/23-25	F_{20} / R_{25}	507	+	++
(IIIS2A)	F_{20} / R_{22}	197	+	++
20-25	F_{20} / R_{25}	567	+	(+)
(IIIS2A & B)	F_{20} / R_{22a}	257	+	(+)

Exons	Primers	Product (bp)	Basilar papilla	Brain
30-31/32-33	F_{30} / R_{33}	230	+	–
(with insert)	F_{30a} / R_{33}	227	+	–
30/31a-33	F_{30} / R_{33}	200	–	+
(without insert)	F_{31a} / R_{33}	197	–	+
30/31-33	F_{30} / R_{33}	284	–	+
(IVS3A & B)	F_{31} / R_{33}	281	–	+

FIG. 1. Alternative splicing of the α_{1D} mRNA in the basilar papilla and the brain. (*A*) Southern blot of PCR products amplified with primers flanking the insert in the I-II loop (exon 9a). Marker sizes in base pairs are indicated on the left. The diagram below of the putative genomic structure (not drawn to scale) depicts exons as rectangles, introns as horizontal lines, and PCR primers as arrows. To amplify all isoforms together, we used primers F_9 and R_{14}. To amplify rare isoforms without interference from more abundant ones, we used exon-specific primers: primer F_{9a} binds across the splice junction of exons 9 and 9a, and primer F_{10} binds across that of exons 9 and 10. The table at the bottom lists product size and occurrence for each splice variant and primer pair. ++, abundant; +, detectable; (+), barely so; –, not detectable. (*B*) Same as *A*, but for the alternative IIIS2 segment (exon 22a). Note the abundance in the basilar papilla of mRNAs with exons for both IIIS2 segments. (*C*) Same as *A*, but for the insert in the IVS2–3 loop (exon 30a). Primer F_{30a} binds across the splice junction of exons 30 and 30a, primer F_{31} binds across that of exons 30 and 31, and primer F_{31a} binds across that of exons 30 and 31a. For the basilar papilla, the lengths of even the minor products were consistent only with splice isoforms containing exon 30a; for the brain, they were consistent only with isoforms lacking exon 30a. Note the abundance in the brain of mRNAs with exons for both IVS3 segments.

SDS under reducing conditions (11) and transferred electrophoretically onto a polyvinylidene difluoride membrane (Immobilon-P, Millipore). A digitonin-soluble membrane fraction was purified from a chicken brain as described (12), except that labeling with radioactive dihydropyridine was omitted. This membrane fraction and crude protein from the basilar papilla were separated and transferred to a membrane as above, except that 4% (wt/vol) polyacrylamide gels were used and methanol was omitted from the transfer buffer. The size markers were β-galactosidase, 116 kDa; myosin, 200 kDa (both in Mark12 wide-range protein standard, NOVEX, San Diego); α- and β-spectrin from human erythrocytes, 220 kDa and 240 kDa; and laminin from basement membrane of Engelbreth-Holm-Swarm mouse sarcoma, about 400 kDa (both from Sigma); they were detected on the membrane with a colloidal-gold solution and a silver enhancing kit (Protogold, Research Diagnostics, Flanders, NJ).

For antibody detection, the membrane was incubated for 1 h in PBS containing 5% (wt/vol) nonfat dried milk and 0.1% (vol/vol) polyoxyethylene sorbitan monolaurate (Tween-20) and washed five times in PBS containing 0.1% (vol/vol) polyoxyethylene sorbitan monolaurate. The membrane was then incubated for 1 h with a 10,000-fold diluted mouse monoclonal antibody against the T7 tag (Novagen) or a 1,000-fold dilution of the affinity-purified antibodies against the α_{1D} subunit in the blocking solution and washed as before. Finally, the membrane was incubated for 1 h with 1,000-fold diluted secondary antibodies raised in sheep against mouse IgG or raised in donkey against rabbit IgG and coupled to horseradish peroxidase (Amersham). After 10 washes, the bound antibodies were detected with SuperSignal Ultra chemiluminescent substrate (Pierce).

RNA Blotting. Polyadenylated RNA was purified from total RNA with oligo(dT) coupled to latex beads (Oligotex, Qiagen). Ten micrograms of poly(A) RNA from the basilar papilla or the brain was separated by electrophoresis through a 0.8% (wt/vol) agarose gel containing 2.2 M formaldehyde, transferred for 4 h to a positively charged nylon membrane by capillary action with 20× SSC (1× SSC is 0.15 M NaCl and 15 mM sodium citrate), and immobilized by ultraviolet irradiation. The RNA size markers were stained on the membrane with a colloidal-gold solution and a silver enhancing kit (Genogold, Research Diagnostics). The poly(A) RNA lanes were hybridized (DIG-Easy Hybe, Boehringer Mannheim) for 16 h at 68°C with digoxigenin-labeled antisense RNA probes synthesized from either the α_{1C} clone pSE1/3–3 or the α_{1D} clones pBr48A, pBr48B, pBr13AL, and pSE152/29–1 (8). The membrane was washed twice for 5 min each at 68°C with a solution of 2× SSC and 0.1% (wt/vol) SDS and twice for 15 min each at 68°C with a solution of 0.1× SSC and 0.1% (wt/vol) SDS. Bound probe was detected with anti-digoxigenin Fab fragments coupled to alkaline phosphatase and the chemiluminescent substrate CDP-Star (Tropix, Bedford, MA).

RESULTS

Alternative Splicing of the α_{1D} mRNA in Hair Cells. In three regions of the ORF, we previously have found extended mismatches between α_{1D} cDNA clones from the basilar papilla and the brain (see figure 3 in ref. 8). The boundaries of these mismatches coincide with exon–intron boundaries in the human α_{1D} gene (13), suggesting that they result from alternative splicing. None of these mismatches starts with GT, the con-

sensus splice-donor dinucleotide, or ends with AG, the consensus splice-acceptor dinucleotide (14), indicating that they are true exons.

The first mismatch occurs in the cytoplasmic loop between repeats I and II (I-II loop), where exon 9a with 26 additional aa is retained between exons 9 and 10 in the basilar papilla, but not in the brain (Fig. 1*A*; exons are numbered according to ref. 13). Next, the second transmembrane segment of the third repeat (IIIS2) is encoded by exon 22a in the basilar papilla and differs by 6 aa from the IIIS2 segment encoded by exon 22 in the brain; the latter is identical to segment IIIS2 in the mammalian α_{1D} cDNAs (Fig. 1*B*). The final mismatch lies in the cytoplasmic loop between the second and third transmembrane segments of the fourth repeat (IVS2–3 loop), where exon 30a, with 10 additional aa, is retained between exons 30 and 31 in the basilar papilla, but not in the brain (Fig. 1*C*). In the bullfrog, *Rana catesbeiana*, we also observed a 10-aa insert with 7 identical residues (ICVAKKKRWL) at the same position in α_{1D} mRNA from saccular hair cells, but not from the brain (data not shown).

We isolated from the chicken's basilar papilla three additional splice variants that shorten the ORF, but observed each only once. The first variant has 12 nt with a stop codon inserted between exons 45 and 46 and encodes an α_{1D} protein of 1,894 aa; the other two diverge after exon 41 or 42 and encode proteins of 1,704 or 1,728 aa, respectively (data not shown; compare figure 3 in ref. 8).

To obtain a better estimate of the relative abundances of the I-II loop, IIIS2, and IVS2–3 splice isoforms, we conducted PCRs with cDNA from the basilar papilla and the brain and analyzed the bulk products. The I-II-loop insert is retained in most α_{1D} mRNAs in the basilar papilla; in the brain, by contrast, it is rare (Fig. 1*A*). Both IIIS2 isoforms are present in both tissues, but exon 22a is more abundant in the basilar papilla, whereas exon 22 predominates in the brain (Fig. 1*B*). Most transcripts in the basilar papilla contain the IVS2–3 insert; in the brain, by contrast, this insert is not detectable (Fig. 1*C*).

From these results, we conclude that α_{1D} mRNA in hair cells consistently bears three modifications due to cell-specific splicing: an insert in the I-II loop (exon 9a), an alternative IIIS2 segment (exon 22a), and an insert in the IVS2–3 loop (exon 30a).

Splice-Acceptor Selection at the I-II-Loop Insert. We took a particular interest in the insert in the I-II loop, a region known to be involved in the channel's modulation (15). We first confirmed that the basilar papilla actually contains α_{1D} protein with the I-II-loop insert. On an immunoblot of crude protein from the basilar papilla, affinity-purified antibodies that specifically recognize this insert detected a single protein with an apparent molecular mass of about 280 kDa (Fig. 2). Perhaps because of glycosylation, this mass exceeds the 245 kDa predicted from the ORF. A protein of the same size was detected by affinity-purified antibodies against another epitope in the I-II loop that is conserved among α_{1D} subunits and by a polyclonal antiserum against the carboxyl terminus of the rat α_{1D} subunit (data not shown).

A comparison of the actual size of the α_{1D} mRNA to that predicted from the composite sequence revealed that intron 9 is spliced out less efficiently than other introns in the basilar papilla. On blots of poly(A) RNA from the basilar papilla and the brain, antisense α_{1D} riboprobes detected species that were 8.9 kb, about 10.5 kb, and 12 kb in length (Fig. 3*A*). The 8.9-kb species, of the size predicted from the composite sequence, is the most abundant in the brain, but the least abundant in the basilar papilla. To isolate the additional 1.6 kb and 3 kb of sequence in the longer species, we conducted PCRs under conditions that favored the amplification of long products with primers that bracketed the entire α_{1D} sequence. Primer pairs that bind on both sides of intron 9—within exons 2 and 37, 2 and 21, 9 and 10, or 9 and 9a—consistently amplified a product of the expected size from the basilar papilla and the brain; in addition, they amplified two products from the basilar papilla that were 1.1 kb and 3.2 kb longer (data not shown). Sequencing these longer PCR products and PCR products from genomic DNA showed that the 3.2-kb segment represents the entire intron 9, with numerous stop codons in every reading frame, whereas the 1.1-kb segment represents the 3′ end of intron 9 (data not shown). These results suggest that all or part of intron 9 often is retained during splicing of α_{1D} pre-mRNAs in the basilar papilla (Fig. 3*B*).

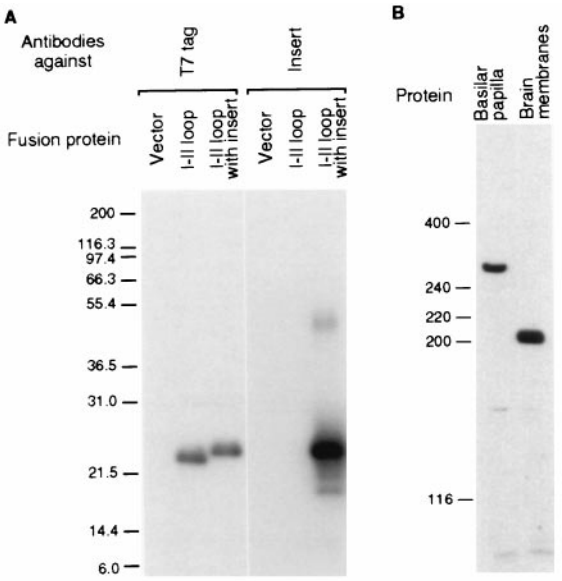

FIG. 2. Presence of the I-II-loop insert in the α_{1D} protein. (*A*) Specificity of antibodies against the I-II loop insert. Blots of crude protein from the bacterial host harboring the expression vector only, of purified fusion protein containing the I-II loop alone, or of purified fusion protein containing the I-II loop with the insert were probed with an antibody against the fusion proteins' T7 tag or with affinity-purified antibodies against the I-II-loop insert. The fusion proteins migrated slower than expected from their predicted masses of 16.4 kDa and 19.5 kDa, respectively. The blot on the right was overexposed to show the lack of binding to other proteins; the band at 47 kDa represents dimeric fusion protein. Marker sizes in kilodaltons are indicated on the left in both panels. (*B*) Sizes of the α_{1D} proteins in the basilar papilla and the brain. A blot of crude protein from three basilar papillae and 20 μg of membrane protein from the brain was probed with the affinity-purified antibodies against the I-II-loop insert. The smaller size of the protein from the brain may reflect proteolysis during purification or may result from synaptic activity (40).

We then inspected the cis-acting splice signals in intron 9. The best match to the consensus of splice-acceptor sites (14) occurs at nucleotide 2113 (Fig. 1 *C* and *D*). Use of this site creates the experimentally observed α_{1D} mRNA with a 1.1-kb insert and a curtailed ORF. In contrast, the acceptor site at the 3′ end of intron 9, which alone gives rise to a full-length ORF, ranks only in the 64th percentile of all candidate splice-acceptor sites in intron 9. We conclude from this finding that the splice acceptor at the 3′ end of intron 9 is insufficient to direct efficient splicing of exons 9 and 9a.

DISCUSSION

Our results demonstrate that the α_{1D} mRNA in hair cells is spliced in a hair-cell-specific manner: most α_{1D} proteins contain a 26-aa insert in the I-II loop, the product of an alternative IIIS2 exon, and a 10-aa insert in the IVS2–3 loop. We do not propose that these splice variants are expressed only in hair cells; the I-II-loop insert, for example, is present in a small fraction of the α_{1D} mRNA in the brain. The relative abundance

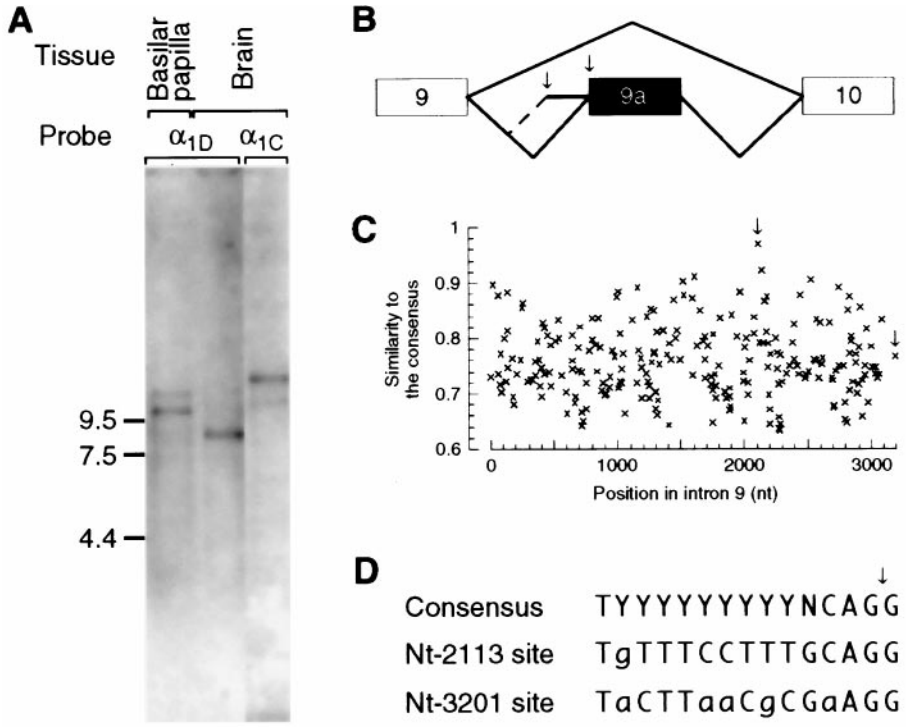

FIG. 3. Splice-acceptor selection at the insert in the I-II-loop. (*A*) Size of the α_{1D} mRNA in the basilar papilla and the brain. Several blots with poly(A) RNA from the basilar papilla or the brain were hybridized with probes for the α_{1D} or the α_{1C} mRNA. The result of one of those experiments is shown; marker sizes in kilobases are indicated on the left. The α_{1D} probes detected species of 8.9 ± 0.09 kb (n = 31), about 10.5 kb (n = 1), and 12 kb (n = 1); the α_{1C} probe revealed species of 11.0 ± 0.14 kb (n = 9) and 13.1 ± 0.13 kb (n = 12). (*B*) Structure of the primary α_{1D} transcript between exons 9 and 10. Brackets indicate how alternative splicing joins exons 9 and 10 or exons 9, 9a, and 10. Arrows in this and the following panel indicate the experimentally observed splice acceptor sites at nucleotide 2113 within intron 9 and at nucleotide 3201 at its 3′ end. (*C*) Consensus profile of splice acceptors in intron 9. The similarity to the consensus matrix for splice acceptors (10, 14) was plotted for all AG dinucleotides in intron 9. (*D*) Alignment of the observed splice acceptors to the consensus sequence. The dinucleotide AG at the intron–exon boundary (arrow) is conserved in almost all known splice acceptors. Y, C or T; N, any base; lowercase letters, mismatch to the consensus.

of these exons in the basilar papilla was confirmed by direct sequencing of bulk PCR products and by exon-specific PCR; the presence of the I-II-loop insert was substantiated additionally by protein immunoblotting. These results together indicate that the composite sequence corresponds to an actual mRNA in hair cells. We have isolated additional splice variants, but these and others we may have missed should be rare in hair cells. We cannot exclude the possibility that some of the observed heterogeneity was a result of contamination from the tegmentum vasculosum during tissue isolation.

The I-II loop of α_1 subunits serves in general as an integration site for Ca^{2+}-channel modulation by the β subunit, by protein kinase C, and by guanine-nucleotide-binding proteins (reviewed in ref. 15); the adjacent IS6 segment contributes to voltage-dependent inactivation (16). The I-II-loop insert in the hair cell's α_{1D} subunit is situated next to the binding site for the β subunit and introduces at least one serine residue (amino acid 472) that is surrounded by four basic residues and therefore is a potential substrate for protein kinases (17). Interestingly, the Ca^{2+} conductance of the turtle's cochlear hair cells is modulated by cAMP-activated protein kinase (18). The I-II-loop insert may affect the channel's modulation, for example by obstructing an effector protein's access, or may alter the channel's properties directly. A homologous insert occurs in α_{1C} subunits in the rabbit's heart, lung, and trachea (19, 20), but its physiological effect is unknown.

The alternative splicing in hair cells of exon 9 to the I-II-loop insert (exon 9a) entails the use of a mediocre splice-acceptor site. About 80 sites within intron 9 match the splice-acceptor consensus better than the site next to exon 9a; indeed, exon 9 is often spliced to the site within intron 9 that most closely resembles the consensus. Productive splicing of the I-II-loop insert may require a cell-specific factor (for a review, see ref. 21) that guides the splice machinery to exon 9a instead of exon 10.

The alternative IIIS2 segment may affect the voltage dependence of activation, even though the amino acid changes are conservative. Homologous exons occur in α_{1C} subunits in rat brain (22), mouse brain (23), and human skin fibroblasts (ref. 24; exons 21 and 22 in ref. 25). The exchange of alternative IIIS2 exons in the α_{1C} subunit alters the voltage dependence of inactivation by dihydropyridines (6). In voltage-gated K^+ channels, mutation of charged residues in the S2 segment changes the voltage dependence of activation (26, 27).

The region between segments IVS2 and IVS4 is noted for its many splice variants in all Ca^{2+} channel α_1 subunits. For example, exons 31 and 31a encode alternative IVS3 segments in the α_{1D} subunit, and exon 32 in the IVS3–4 loop is optional (28–30); alternative splicing of the IVS3–4 segment in the α_{1A} subunit changes the channel's kinetic properties (7). The IVS2–3 insert that we found in the α_{1D} subunit has no precedent. The occurrence of this insert in hair cells, but not in the brain, of both the chicken and the bullfrog suggests an important role in shaping the channel's behavior.

Expression of the α_{1D} subunit with the various combinations of these three alternative exons will allow us to investigate whether they confer the physiological properties of the native Ca^{2+} channel in hair cells. However, we expect the channel's properties to depend as well on the specific complement of auxiliary subunits, which might themselves be spliced in a cell-specific manner.

We did not observe any differences between the α_{1D} subunits of hair cells and the brain in several regions where alterations would be expected to change channel properties. The S4 segments, the voltage sensors of voltage-gated cation channels (31), are identical. The IS3 segment and the IS3–4

loop are identical. These regions are critical for fast activation of the α_{1C} and slow activation of the α_{1S} subunit (32); as might be expected, the α_{1D} sequence resembles more closely the α_{1C} than the α_{1S} sequence. Finally, the α_{1D} subunit in hair cells retains a Ca^{2+}-binding EF-hand motif carboxyl to segment IVS6. The region containing the homologous motif in the α_{1C} subunit has been proposed to confer Ca^{2+}-dependent inactivation (33); more recently, however, Ca^{2+} inactivation has been localized instead to a stretch of about 140 aa carboxyl to the EF-hand (34, 35). Except for about 15 residues, this stretch is virtually identical between the α_{1C} and the α_{1D} subunits. Constructing chimeras between these two may make it possible to determine the roles of the EF-hand and the adjacent sequences in Ca^{2+}-dependent inactivation.

Hair cells provide a convenient system in which to study the tonic release of neurotransmitter, for they lend themselves to patch clamping, capacitance measurements, and Ca^{2+} imaging (36–39). Because the Ca^{2+} channels that control Ca^{2+} entry at the hair cell's presynaptic sites are homogeneous, we can correlate their unusual pharmacological and electrophysiological properties and their molecular structure. Our results support the hypothesis that these properties stem, at least in part, from cell-specific splicing of the mRNA for an L-type α_{1D} subunit.

We thank Drs. D. Nelson and T. Snutch for the antiserum against the rat α_{1D} subunit, Dr. P. Gillespie and Ms. R. Orman for advice, and Drs. P. Farnham and J. Imredy, as well as members of our research group, for comments on drafts of the manuscript. Begun at University of Texas Southwestern Medical Center, this research was supported by National Institutes of Health Grant DC00317. R.K. was an Associate and A.J.H. is an Investigator of Howard Hughes Medical Institute.

1. Lewis, R. S. & Hudspeth, A. J. (1983) *Nature (London)* **304,** 538–541.
2. Zidanic, M. & Fuchs, P. A. (1995) *Biophys. J.* **68,** 1323–1336.
3. Hudspeth, A. J. (1989) *Nature (London)* **341,** 397–404.
4. Hofmann, F., Biel, M. & Flockerzi, V. (1994) *Annu. Rev. Neurosci.* **17,** 399–418.
5. Catterall, W. A. (1995) *Annu. Rev. Biochem.* **64,** 493–531.
6. Soldatov, N. M., Bouron, A. & Reuter, H. (1995) *J. Biol. Chem.* **270,** 10540–10543.
7. Lin, Z., Haus, S., Edgerton, J. & Lipscombe, D. (1997) *Neuron* **18,** 153–166.
8. Kollmar, R., Montgomery, L. G., Fak, J., Henry, L. J. & Hudspeth, A. J. (1997) *Proc. Natl. Acad. Sci. USA* **94,** 14883–14888.
9. Gillespie, P. G. & Hudspeth, A. J. (1993) *Proc. Natl. Acad. Sci. USA* **90,** 2710–2714.
10. Quandt, K., Frech, K., Karas, H., Wingender, E. & Werner, T. (1995) *Nucleic Acids Res.* **23,** 4878–4884.
11. Harlow, E. & Lane, D. (1988) *Antibodies: A Laboratory Manual* (Cold Spring Harbor Lab. Press, Cold Spring Harbor, NY).
12. Hell, J. W., Westenbroek, R. E., Warner, C., Ahlijanian, M. K., Prystay, W., Gilbert, M. M., Snutch, T. P. & Catterall, W. A. (1993) *J. Cell Biol.* **123,** 949–962.
13. Yamada, Y., Masuda, K., Li, Q., Ihara, Y., Kubota, A., Miura, T., Nakamura, K., Fujii, Y., Seino, S. & Seino, Y. (1995) *Genomics* **27,** 312–319.
14. Senapathy, P., Shapiro, M. B. & Harris, N. L. (1990) *Methods Enzymol.* **183,** 252–278.
15. Dunlap, K. (1997) *Nature (London)* **385,** 394–395, 397.
16. Zhang, J.-F., Ellinor, P. T., Aldrich, R. W. & Tsien, R. W. (1994) *Nature (London)* **372,** 97–100.
17. Pinna, L. A. & Ruzzene, M. (1996) *Biochim. Biophys. Acta* **1314,** 191–225.
18. Ricci, A. J. & Fettiplace, R. (1997) *J. Physiol.* **501,** 111–124.
19. Biel, M., Ruth, P., Bosse, E., Hullin, R., Stühmer, W., Flockerzi, V. & Hofmann, F. (1990) *FEBS Lett.* **269,** 409–412.
20. Biel, M., Hullin, R., Freundner, S., Singer, D., Dascal, N., Flockerzi, V. & Hofmann, F. (1991) *Eur. J. Biochem.* **200,** 81–88.
21. Chabot, B. (1996) *Trends Genet.* **12,** 472–478.
22. Snutch, T. P., Tomlinson, W. J., Leonard, J. P. & Gilbert, M. M. (1991) *Neuron* **7,** 45–57.
23. Ma, W.-J., Holz, R. W. & Uhler, M. D. (1992) *J. Biol. Chem.* **267,** 22728–22732.
24. Soldatov, N. M. (1992) *Proc. Natl. Acad. Sci. USA* **89,** 4628–4632.
25. Soldatov, N. M. (1994) *Genomics* **22,** 77–87.
26. Planells-Cases, R., Ferrer-Montiel, A. V., Patten, C. D. & Montal, M. (1995) *Proc. Natl. Acad. Sci. USA* **92,** 9422–9426.
27. Seoh, S.-A., Sigg, D., Papazian, D. M. & Bezanilla, F. (1996) *Neuron* **16,** 1159–1167.
28. Perez-Reyes, E., Wei, X., Castellano, A. & Birnbaumer, L. (1990) *J. Biol. Chem.* **265,** 20430–20436.
29. Hui, A., Ellinor, P. T., Krizanova, O., Wang, J.-J., Diebold, R. J. & Schwartz, A. (1991) *Neuron* **7,** 35–44.
30. Ihara, Y., Yamada, Y., Fujii, Y., Gonoi, T., Yano, H., Yasuda, K., Inagaki, N., Seino, Y. & Seino, S. (1995) *Mol. Endocrinol.* **9,** 121–130.
31. García, J., Nakai, J., Imoto, K. & Beam, K. G. (1997) *Biophys. J.* **72,** 2515–2523.
32. Nakai, J., Adams, B. A., Imoto, K. & Beam, K. G. (1994) *Proc. Natl. Acad. Sci. USA* **91,** 1014–1018.
33. de Leon, M., Wang, Y., Jones, L., Perez-Reyes, E., Wei, X., Soong, T. W., Snutch, T. P. & Yue, D. T. (1995) *Science* **270,** 1502–1506.
34. Soldatov, N. M., Zühlke, R. D., Bouron, A. & Reuter, H. (1997) *J. Biol. Chem.* **272,** 3560–3566.
35. Zhou, J., Olcese, R., Qin, N., Noceti, F., Birnbaumer, L. & Stefani, E. (1997) *Proc. Natl. Acad. Sci. USA* **94,** 2301–2305.
36. Roberts, W. M., Jacobs, R. A. & Hudspeth, A. J. (1990) *J. Neurosci.* **10,** 3664–3684.
37. Issa, N. P. & Hudspeth, A. J. (1994) *Proc. Natl. Acad. Sci. USA* **91,** 7578–7582.
38. Parsons, T. D., Lenzi, D., Almers, W. & Roberts, W. M. (1994) *Neuron* **13,** 875–883.
39. Tucker, T. & Fettiplace, R. (1995) *Neuron* **15,** 1323–1335.
40. Hell, J. W., Westenbroek, R. E., Breeze, L. J., Wang, K. K. W., Chavkin, C. & Catterall, W. A. (1996) *Proc. Natl. Acad. Sci. USA* **93,** 3362–3367.